

# Taming molecular beams

The motion of neutral molecules in a beam can be manipulated with inhomogeneous electric and magnetic fields. Static fields can be used to deflect or focus molecules, whereas time-varying fields can be used to decelerate or accelerate beams of molecules to any desired velocity. We review the possibilities that this molecular-beam technology offers, ranging from ultrahigh-resolution spectroscopy using molecular fountains to novel crossed-beam scattering experiments.

SEBASTIAAN Y. T. VAN DE MEERAKKER<sup>1</sup>,  
HENDRICK L. BETHLEM<sup>1,2</sup> AND GERARD MEIJER<sup>1\*</sup>

<sup>1</sup>Fritz-Haber-Institut der Max-Planck-Gesellschaft, Faradayweg 4-6, D-14195 Berlin, Germany

<sup>2</sup>Laser Centre Vrije Universiteit, De Boelelaan 1081, NL-1081 HV Amsterdam, The Netherlands

\*e-mail: meijer@fhi-berlin.mpg.de

Atomic and molecular beams have played central roles in many experiments in physics and chemistry—from seminal tests of fundamental aspects of quantum mechanics to molecular reaction dynamics—and have found a wide range of applications<sup>1</sup>. Nowadays, sophisticated laser-based detection methods exist to selectively detect molecules in specific quantum states. In the early days, quantum-state selectivity in the detection process was achieved by inhomogeneous magnetic and/or electric field sections to influence the trajectories of the particles to the detector. This was the approach used by Gerlach and Stern<sup>2</sup> in 1922, and the key concept of their experiment, the sorting of quantum states through space quantization, has been extensively used ever since. The original experimental geometries were devised to create strong magnetic or electric field gradients on the beam axis to efficiently deflect particles<sup>3</sup>. Later, both magnetic<sup>4,5</sup> and electric<sup>6</sup> field geometries were designed to focus particles in selected quantum states onto the detector. For example, an electrostatic quadrupole focuser was used to couple a beam of ammonia molecules into a microwave cavity. The resulting inverted population distribution led to the invention of the maser by Gordon *et al.*<sup>7,8</sup> in 1954–1955. By using several multipole focusers in succession, with interaction regions with electromagnetic radiation in between, versatile set-ups to unravel the quantum structure of atoms and molecules were developed. In scattering experiments, multipole focusers in combination with electrostatic orientation fields were exploited to study steric effects, ‘to aim the molecular arrow’<sup>9</sup>. Variants of these methods were implemented in many laboratories, and have yielded a wealth of detailed information on stable molecules, radicals and molecular complexes, thereby contributing enormously to our present understanding of intramolecular and intermolecular forces.

The manipulation of beams of atoms and molecules with electric and magnetic fields is thus about as old as the field of atomic and molecular beams itself, and it has actually been crucial for the success of the latter field. However, this manipulation exclusively

involved the transverse motion of the molecules. Experiments to manipulate the longitudinal motion of molecules in a beam were considered and tried in the 1950s and 1960s. Electric field deceleration of neutral molecules was first attempted by John King at Massachusetts Institute of Technology to produce a slow ammonia beam to obtain a maser with an ultranarrow linewidth. In the physical chemistry community, the experimental efforts of Lennard Wharton, to demonstrate electric field acceleration of a molecular beam, are much better known. At the University of Chicago, he constructed an 11-m-long molecular beam machine for the acceleration of LiF molecules in high-field-seeking states from 0.2 to 2.0 eV, aiming to use these high-energy beams for reactive scattering studies<sup>10</sup>. Both of these experiments were unsuccessful, and were not continued after the PhD projects were finished<sup>11,12</sup>.

It was only in 1999 that it was experimentally demonstrated that appropriately designed arrays of electric fields in a so-called ‘Stark decelerator’ can indeed be used to influence and control the longitudinal (forward) velocity of the molecules in a beam, for example, to decelerate a beam of neutral polar molecules<sup>13</sup>. In the same year, time-varying electric-field-gradient slowing of Cs atoms was demonstrated by Gould and co-workers<sup>14</sup>. Since then a variety of decelerators have been designed and built, ranging in size from decelerators integrated on a chip to several-metre-long decelerators, and have made a whole variety of new experiments possible. For instance, when the molecules are decelerated to a standstill, they can be loaded and confined in traps. This enables the observation of molecules in complete isolation from their environment for times up to several seconds, and enables the investigation of molecular properties and their interactions in unprecedented detail. The subject of this review is how full control over the three-dimensional motion of neutral molecules can be achieved, and how these ‘tamed’ molecular beams can be used to advantage in a variety of novel experiments.

## THE STARK DECELERATOR AND TRAP

The Stark decelerator for neutral polar molecules is the equivalent of a linear accelerator for charged particles. Whereas in charged-particle accelerators, the force that is exerted on a particle depends on its charge and the electric field strength, in a Stark decelerator, the dipole (charge times separation) in a polar molecule is acted on by electric field gradients. This quantum-state-specific

## Box 1: Molecular beams

A molecular beam is formed by letting a gas pass from a high-pressure container through a small orifice into an evacuated chamber, that is, by a controlled leak, as schematically shown in Fig. B1. If the hole is much smaller than the mean free path of the gas, molecules will every now and then escape from the container through the hole without undergoing collisions. In this case, the velocity distribution as well as the distribution over the internal degrees of freedom of the molecules (rotation, vibration) in the beam is the same as that in the container. These beams are said to be effusive. Although the most probable velocity of molecules in an effusive beam originating from a room-temperature container is a few hundred metres per second, a small fraction of the molecules will have velocities below  $30 \text{ m s}^{-1}$ . Using either curved electrostatic guides<sup>79–82</sup> or a mechanical selector—a series of rotating blades<sup>83</sup>—these slow molecules can be filtered out of the effusive beam and used for experiments<sup>84</sup>. Higher fluxes of slow and internally colder molecules can be obtained when the effusive beam is extracted from a cryogenic container.<sup>85,86</sup>

If the pressure in the container is raised or if the size of the hole is increased, the mean free path of the gas becomes smaller than the orifice. In this case, molecules escaping through the hole collide frequently, and adiabatic cooling of all degrees of freedom takes place in the expansion region. The total energy available per molecule in the gas in the container is converted into kinetic energy (directed flow), leading to supersonic beams of internally cold molecules<sup>87</sup>. The terminal temperature in the beam is limited by the formation of clusters, which is reduced when the molecule of interest is expanded in a dilute mixture with a noble gas. When these beams are operated in a pulsed mode, pumping requirements are less severe and millimetre-sized orifices can be used. In these pulsed beams, densities of  $10^{13} \text{ molecules cm}^{-3}$  at translational temperatures below 1 K can be obtained. The rotational temperature in the beam is normally close to the translational temperature, whereas the vibrational degrees of freedom are known to cool considerably less well. The velocity of the beam is dictated by the mass of the carrier gas and by the temperature and pressure of the source<sup>88</sup>. Molecules seeded in a room-temperature Kr (Xe) expansion move at a terminal velocity of about  $440 \text{ m s}^{-1}$  ( $330 \text{ m s}^{-1}$ ). These seeded pulsed beams are ideal starting points for Stark, Zeeman and optical deceleration experiments.

force is typically eight orders of magnitude smaller than the forces that are typically used in charged-particle accelerators, but nevertheless suffices to achieve complete control over the motion of polar molecules using techniques akin to those used to control charged particles.

In a Stark decelerator, the longitudinal velocity of a beam of polar molecules (see Box 1 for details) is manipulated using an array of longitudinally inhomogeneous electric fields as is shown in Fig. 1. At a given time, the even-numbered stages are switched to high voltage and the odd-numbered stages are grounded. Molecules in low-field-seeking states that approach the plane of the first electrodes experience the increasing electric field as a potential hill, and will lose kinetic energy on the upward slope of the potential hill. When the molecule leaves the region of high field again, however, it will regain the same amount of kinetic energy. The acceleration on the downward slope of the hill can be avoided by switching off the electric field when the molecule has reached a

Rather than grabbing with fields onto the molecules, other techniques to produce slow molecular beams have been developed. In a crossed or counterpropagating beam set-up, the kinetic energy transfer in collisions<sup>89</sup> or reactions<sup>90</sup> between molecules can be exploited to produce slow or stationary molecules. Molecules can also be slowed and loaded into a magnetic trap by introducing a molecular beam into a cryogenic buffer gas<sup>91</sup>. Mechanical methods, originally pioneered by Moon and co-workers in the 1970s to accelerate a molecular beam<sup>92</sup>, have been developed as well. For instance, the laboratory velocity of a molecular beam can be lowered by a nozzle that is mounted on a back-spinning rotor<sup>93,94</sup> or by elastic reflection from a receding substrate<sup>95</sup>.

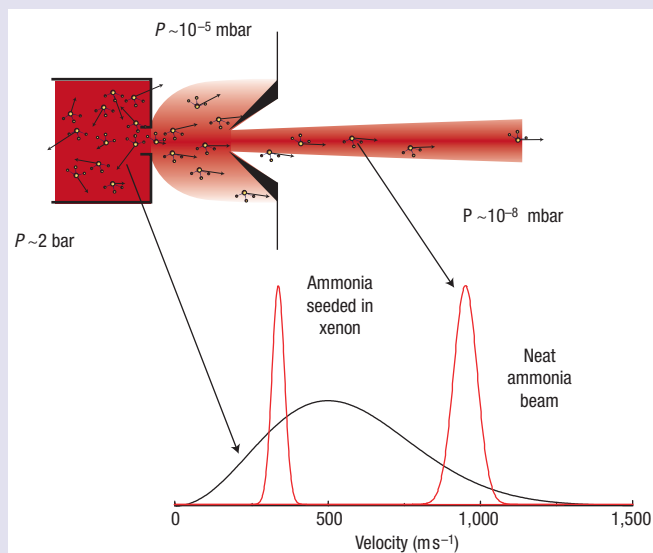


**Figure B1** Schematic view of a supersonic expansion. A high-pressure gas is expanded through a small hole into vacuum. Lower panel: The velocity distribution of room-temperature ammonia molecules in the container and in the supersonic beam. By using a noble gas as a carrier, the velocity distribution is further narrowed. The terminal velocity of the ammonia molecules will then be the same as that of the carrier gas.

position that is close to the top of the first potential hill. At the same time, the sets of electrodes that were grounded are switched to high voltage. Consequently, the molecule will find itself again in front of a potential hill and will again lose kinetic energy when climbing this hill. When the molecule has reached the high electric field region, the voltages are switched back to the original configuration. By repeating this process many times, the velocity of the molecule can be reduced to an arbitrarily low value.

The amount of kinetic energy that is lost per stage depends on the exact position of the molecule at the time that the fields are being switched. The computer-controlled high-voltage pulses thus determine the final velocity of the molecule. A second important property of the Stark decelerator is that, like in charged-particle accelerators, the deceleration process is phase stable. This means that the process can be described as the trapping of a packet of molecules in a travelling potential well<sup>15</sup>. Hence, the deceleration process does not work only for one molecule in the beam, but it

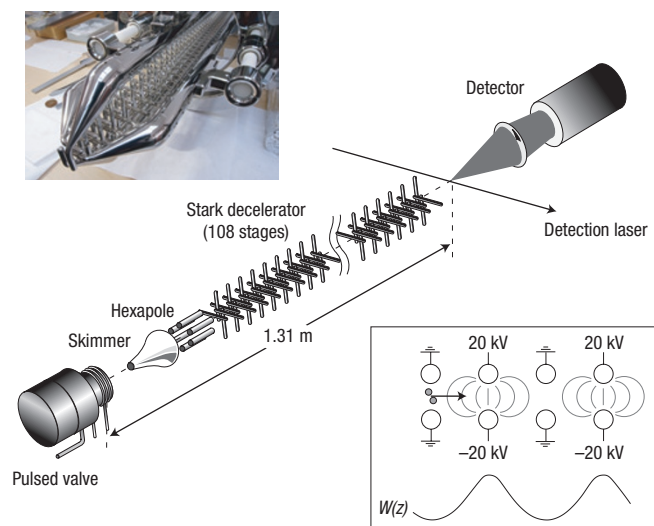


**Figure 1** Scheme of the set-up for a Stark-deceleration experiment. A pulsed molecular beam is produced and passes through a skimmer, hexapole and Stark decelerator into the detection region. The electric field stages of the decelerator are composed of two opposing electrodes that are connected to power supplies of opposite polarity. Alternating rods are connected to each other. Reprinted with permission from ref. 78. © 2006 Annual Reviews. Bottom inset: The potential energy  $W(z)$  of a molecule that is in a low-field-seeking quantum state—that is, a molecule that gains Stark energy when flying into an increasing electric field—as a function of the position  $z$  along the beam axis. Top inset: A photograph of one of the decelerators that is operational in our laboratory. Reprinted with permission from ref. 32. © 2007 APS.

works for all molecules that at the entrance of the decelerator have a longitudinal position and velocity within a certain interval<sup>15–18</sup> (see Box 2 for details). It is also required that the molecules keep together in the transverse direction. Molecules in low-field-seeking states stay transversely confined to the molecular beam axis as the electric field is always lower on this axis than on the electrodes. Together, these three properties enable us to decelerate (or to accelerate) part of the beam to any desired velocity, while keeping the selected part of the beam together as a compact packet.

The methods described above work only for molecules in a low-field-seeking quantum state, and have so far been applied to the molecules CO( $a^3\Pi$ ) (ref. 13), ND<sub>3</sub> (ref. 19), OH (refs 20,21), OD (ref. 22), NH( $a^1\Delta$ ) (ref. 23), H<sub>2</sub>CO (ref. 24) and SO<sub>2</sub> (ref. 25). High-field-seeking molecules are deflected from the molecular beam axis and will eventually be lost. This fundamental problem can be overcome by using alternating gradient focusers<sup>26,27</sup>, and has been demonstrated for high-field-seeking metastable CO molecules<sup>28</sup>, ground-state YbF molecules<sup>29</sup> and benzonitrile<sup>30</sup>.

After exiting the decelerator, the decelerated packets of molecules can be directly used for experiments, or they can be coupled into a variety of elements where they can be manipulated further. Most notably, the molecules can be loaded into traps or into storage rings. The first electrostatic trapping of polar molecules was demonstrated in 2000 using Stark-decelerated ND<sub>3</sub> molecules<sup>19</sup>. Later, the electrostatic trapping technique was applied to the molecules OH (ref. 21), OD (ref. 22), metastable CO (ref. 31) and metastable NH (ref. 32).

The first electrostatic traps for polar molecules had a quadrupole geometry, as was originally proposed by Wing for Rydberg atoms<sup>33</sup>. Traps with other field geometries have been developed and tested as well. A four-electrode trap geometry

that combines a dipole, quadrupole and hexapole field has been tested using decelerated ND<sub>3</sub> molecules. By applying different voltages to the electrodes, a double-well or a doughnut trapping potential can be created<sup>34</sup>. Confinement of Stark-decelerated OH radicals in combined magnetic and electric fields has recently been demonstrated. An electric field was superimposed on a magnetic field to create an overall magnetoelectric trapping potential<sup>35</sup>.

Here, the performance of the Stark decelerator and electrostatic quadrupole trap is illustrated using the OH ( $X^2\Pi_{3/2}$ ,  $J = 3/2$ ) radical as a model species. A typical time-of-flight (TOF) profile of OH radicals exiting the decelerator is shown in Fig. 2a. The undecelerated part of the beam arrives in the detection region about 3 ms after its production. In the TOF profile, a rich oscillatory structure is observed that results from a modulation of the phase-space distribution of the beam in the decelerator<sup>17</sup>. The hole in the beam profile that results from the removal of the packet of molecules that is decelerated is indicated by the vertical arrow. This packet is split off from the original beam pulse, and arrives in the detection region at later times.

When the packet of molecules is decelerated to near standstill, it can be loaded into the electrostatic quadrupole trap by applying voltages asymmetrically on the three trap electrodes. A potential hill in the trap is created that is higher than the remaining kinetic energy of the molecules. The molecules therefore come to a standstill near the centre of the trap. Then, the voltages on the trap electrodes are switched into the ‘trapping geometry’ to create a (nearly) symmetric 500-mK-deep potential well. A typical TOF profile that is obtained for OD radicals is shown in Fig. 2b.

The molecules mainly leave the trap through collisions with particles in the residual gas in the vacuum chamber, or through absorption of blackbody radiation from the (room-temperature) surroundings<sup>22</sup>.

## THE ZEEMAN, RYDBERG AND OPTICAL DECELERATORS

Inspired in part by the manipulation of polar molecules with electric fields, a magnetic analogue of the Stark decelerator has recently been developed. Deceleration based on the magnetic interaction enables the manipulation of a wide range of atoms and molecules to which the Stark deceleration technique cannot be applied. The required rapid switching of the magnetic fields originally posed a significant experimental challenge. The Zeeman deceleration technique was first experimentally demonstrated by the deceleration of ground-state H and D atoms using initially six<sup>36,37</sup> and later twelve<sup>38</sup> pulsed magnetic field stages; a scheme of the original experimental set-up is shown in Fig. 3a. The deceleration stages consist of 7.8-mm-long solenoids of insulated copper wire in which magnetic fields up to 1.5 T are achieved. The coil design provides a cylindrically symmetric transverse restoring force to the molecular beam axis. When the current through the coils is switched, rise-and-fall times of the magnetic pulses as short as 5  $\mu$ s are achieved. These experiments demonstrate the possibility of switching magnetic fields fast enough to enable deceleration and that the deceleration process is subject to phase stability. The Zeeman deceleration technique has also been applied to decelerate metastable Ne atoms<sup>39</sup> in an 18-stage decelerator. Using electromagnet coils that are encased in magnetic steel shells with Permenur discs, even higher magnetic field densities of 3.6 T are achieved. Recently, the deceleration of metastable Ne atoms<sup>40</sup> and oxygen molecules<sup>41</sup> to velocities as low as 50 m s<sup>-1</sup> using 64 stages has been reported.

Compared with the polar molecules discussed thus far, atoms or molecules in a Rydberg state offer a much larger electric dipole moment. Hence, these particles can be manipulated using only modest electric field strengths in a single, or a few electric field

## Box 2: Phase stability

In analogy to the operation of linear accelerators for charged particles, the concept of phase stability is essential to the operation of Stark, Zeeman and optical decelerators. Phase stability is the reason that these decelerators actually work. It is discussed in more detail below for a Stark decelerator.

In a Stark decelerator, the voltages that are applied to the electric field stages are switched such that they are synchronous with a hypothetical molecule, aptly referred to as the ‘synchronous’ molecule, flying on the molecular beam axis. Molecules that are slightly ahead of the synchronous molecule will be decelerated more than the synchronous molecule, whereas molecules that are slightly behind the synchronous molecule will be decelerated less. As a consequence, molecules with a slightly different longitudinal position and velocity from that of the synchronous molecule experience a force towards the synchronous molecule and will oscillate around it. The position of the synchronous molecule with respect to the electrodes at high voltage as the fields are being switched—how far the molecule has entered the field—is expressed in terms of a ‘phase angle’,  $\phi_0$ . When this phase is close to  $90^\circ$ , the deceleration per stage is large, but the longitudinal velocity and position spread of the molecules that will be accepted in the deceleration process is small. When  $\phi_0$  is small, the acceptance is large but the deceleration per stage is small<sup>16</sup>.

In the transverse direction, molecules experience a restoring force towards the beam axis because the electric fields are higher at the electrodes than on the molecular beam axis. This focusing force strongly depends on the exact position of the molecule along the molecular beam axis. Close to the electrodes at high voltage, the transverse focusing is strong, whereas the transverse focusing is small close to the electrodes at ground potential. The oscillatory motion of molecules around the synchronous molecule results in a time-dependent transverse force that can result in unstable trajectories through the decelerator<sup>96</sup>.

In Fig. B2, the six-dimensional acceptance, that is, the product of the position and velocity spread of molecules in each direction that is accepted by the decelerator, is shown as a function of the phase angle for two different operation modes of the decelerator. The acceptance that is obtained from numerical trajectory simulations taking the true force on the molecules into account is given as data points, which are connected by straight line segments. The acceptance that results from the combined model for the longitudinal<sup>16</sup> and transverse<sup>96</sup> motion of molecules in a Stark decelerator, which neglects any coupling between the motion in each orthogonal direction, is given by the smooth curves. In the conventional operation mode of a Stark decelerator, referred to as  $s = 1$  (ref. 17), each deceleration stage is used to remove kinetic energy from the molecules. It is seen that the actual acceptance of the decelerator is much lower than the model prediction, in particular for phase angles below  $70^\circ$ ; the

instabilities that result from the coupling between the longitudinal and transverse motion are severe, and can limit the efficiency. The motions can be uncoupled by using only every third stage for deceleration, whereas the intermediate stages are used for transverse focusing. The performance of the decelerator in this so-called  $s = 3$  mode<sup>17</sup> follows the model prediction much better, and a significantly higher phase-space acceptance can be achieved.

In Stark and Zeeman decelerators, phase stability is ensured by repeatedly switching between two different static configurations, thereby confining the molecules in an effective travelling potential well. This is fundamentally different from the situation in the optical Stark decelerator, where genuine travelling wells are present. The trapping of polar molecules in genuine travelling potential wells closely above a microstructured electrode array has recently been demonstrated<sup>97</sup>.

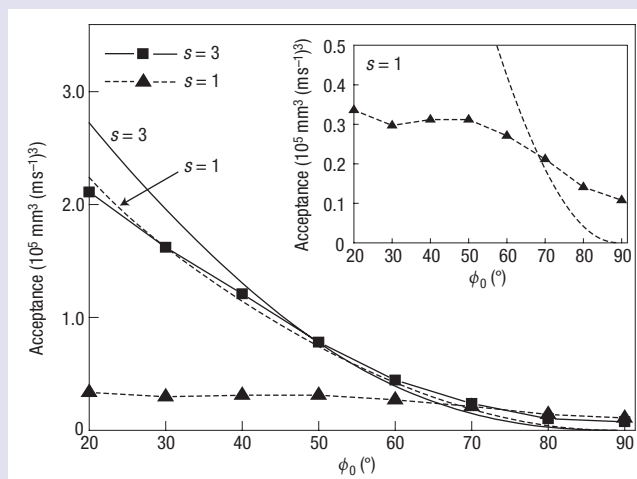


**Figure B2** The six-dimensional phase-space acceptance of a Stark decelerator. The acceptance that results from numerical trajectory simulations as a function of the phase angle (triangles for  $s = 1$  and squares for  $s = 3$ ), together with the model prediction (dashed line for  $s = 1$  and solid line for  $s = 3$ ). The simulations are carried out for OH radicals in the  $X^2 \Pi_{3/2}$ ,  $J = 3/2$ ,  $M\Omega = -9/4$ ,  $f$  state that propagate through a Stark decelerator of variable length. The decelerator is operated with 40 kV voltage difference on opposing electrodes. The electrodes have a diameter of 4.50 mm, are placed at a centre-to-centre distance  $L = 8.25$  mm from each other and leave a  $3 \times 3$  mm<sup>2</sup> area around the beam axis. For each simulation, the length of the decelerator is chosen to slow down the synchronous molecule from 550 to 180 m s<sup>-1</sup>, to exclude loss of molecules due to excessive transverse focusing at low velocities. This is expected below 50 m s<sup>-1</sup> for  $s = 1$  and below 150 m s<sup>-1</sup> for  $s = 3$ .

stages. Energy level crossings in the dense Rydberg manifold limit the magnitude of the electric field strengths that can actually be applied. The electric field manipulation of atoms and molecules in high Rydberg states has been pioneered using H<sub>2</sub> molecules<sup>42</sup> and Ar atoms<sup>43</sup>. Using a Rydberg decelerator, H atoms could be stopped and electrostatically trapped in two<sup>44</sup> or three<sup>45</sup> dimensions. The short lifetimes of Rydberg states inherently limit the time that is available to store and study the particles in a trap. If fluorescence to the ground state is the dominant decay process, however, cold

samples of ground-state atoms or molecules can be produced using this method. As all atoms and molecules possess Rydberg states, this may provide a general route to cold samples of atoms and molecules.

Optical fields provide another general method to manipulate the motion of neutral particles. An intense optical field will polarize and align molecules<sup>46</sup>. In a laser focus, the polarized molecules will experience a force that is proportional to the gradient of the laser intensity, which can be used to focus and trap them. This

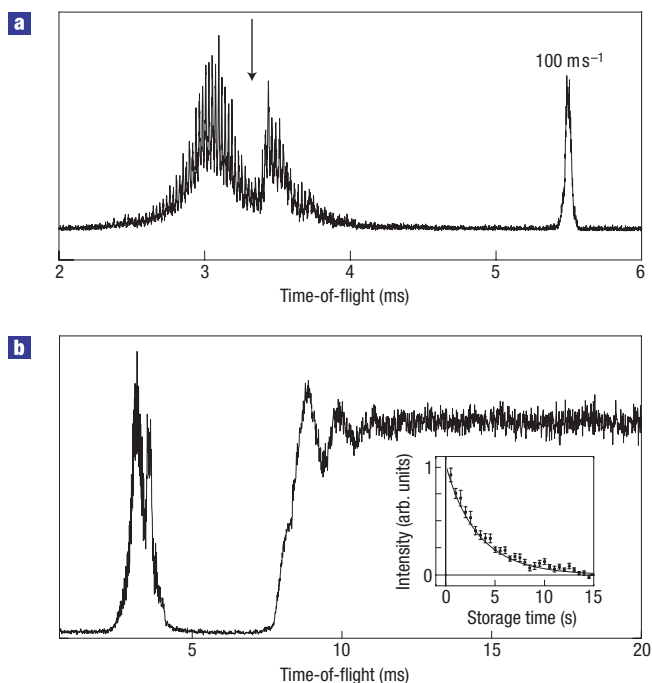


**Figure 2** Stark-decelerated and trapped hydroxyl radicals. **a**, Observed TOF profile of a molecular beam of OH radicals in the  $X^2 \Pi_{3/2}(v=0, J=3/2, f, F=2)$  level exiting the Stark decelerator. The molecular beam has a mean velocity of  $370 \text{ m s}^{-1}$  and the decelerator is programmed to slow down a packet of molecules from 370 to  $100 \text{ m s}^{-1}$ . **b**, Observed TOF profile when a packet of OD molecules is slowed down to standstill and confined in an electrostatic quadrupole trap. Inset: The signal of the trapped OD radicals on a 15 s timescale. Reprinted with permission from ref. 22. © 2007 APS.

was experimentally demonstrated by focusing<sup>47</sup> or deflecting<sup>48</sup> a beam of  $\text{CS}_2$  molecules using a high-intensity pulsed laser beam. Optical forces have also been used to reduce the translational energy of molecular beams<sup>49</sup>. Benzene molecules were decelerated from  $320$  to  $295 \text{ m s}^{-1}$ , while at the same time the xenon carrier gas was decelerated from  $320$  to  $310 \text{ m s}^{-1}$ , illustrating the generality of this method. Rather than using a single laser beam, much higher forces can be generated by using two near-counterpropagating laser beams as shown in Fig. 3b. The two laser beams will interfere to create a so-called optical lattice. Such a lattice forms a periodic array of potential wells for polarizable atoms and molecules. By carefully controlling the frequency difference between the two laser beams, the lattice can be made to move at the same velocity as the molecules in the molecular beam. By slowly lowering the velocity of the lattice, molecules can be decelerated to any given velocity<sup>50</sup>. In this so-called optical Stark decelerator, the chirp of the laser beams needs to be very well controlled, which, in combination with the high intensities, is an experimental challenge. A simpler scheme was recently implemented using a constant frequency offset between the two laser beams such that the lattice moves with a velocity slightly below that of a molecular beam<sup>51</sup>. With a suitable choice of parameters, the molecules make exactly a half oscillation within the optical potential. In this way, NO molecules were decelerated from  $400$  to  $270 \text{ m s}^{-1}$ .

## APPLICATIONS

The control over the motion and orientation of molecules by external fields offers a multitude of new possibilities for precision

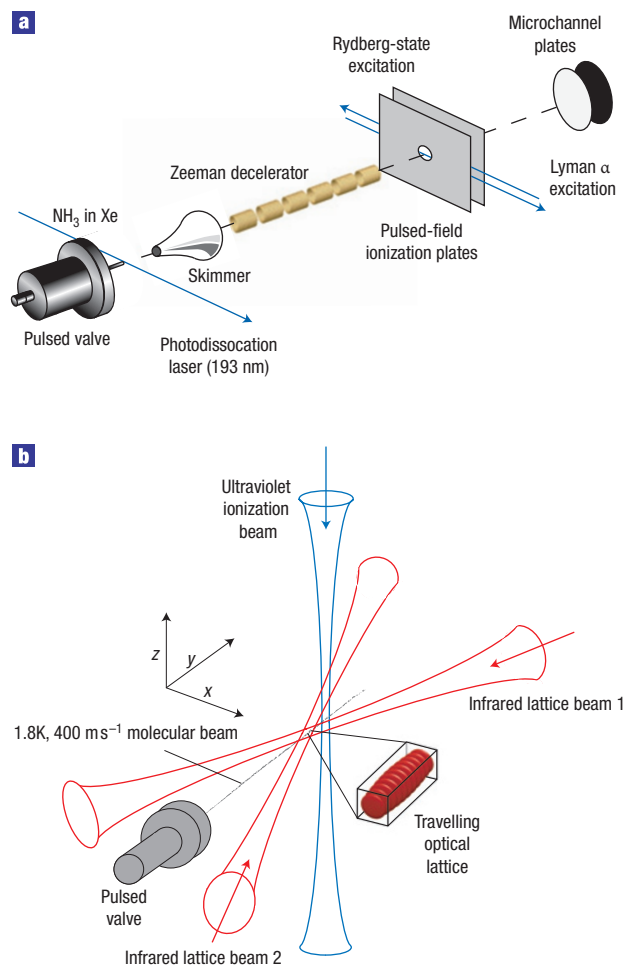


**Figure 3** Scheme of the Zeeman and optical Stark decelerator. **a**, The Zeeman decelerator as used by Vanhaecke *et al.*<sup>36</sup> consisting of six solenoids of insulated copper wire. The decelerator was used to slow down seeded beams of H and D atoms. Reprinted with permission from ref. 36. © 2007 APS. **b**, The optical Stark decelerator as used by Fulton *et al.*<sup>51</sup>. An optical lattice is created by crossing two intense pulsed laser beams. The two laser beams have a slightly different frequency, such that the optical lattice has a velocity that is matched to that of the molecular beam. The molecules are detected by ionizing them using a third laser beam.

studies of molecular properties and interactions. Over the past few years, a number of experiments have been carried out that demonstrate this. These experiments can be separated into three distinct classes: beam collision studies, spectroscopic studies and experiments on molecules that are confined in traps.

Collisions between molecules are highly sensitive to their relative velocity, in particular at low velocities where the kinetic energy of the molecules is comparable to the rotational energy level splitting in the collision complex. At these energies, translational energy can be transferred into rotational energy, effectively binding the molecules transiently together. Long-living excitations of the collision complex show up as sharp resonances in the collision-energy dependence of the scattering cross-sections<sup>52–54</sup>. Stark-decelerated molecular beams are well suited for crossed-beam scattering experiments, as has been demonstrated recently by scattering a Stark-decelerated beam of OH radicals with a conventional beam of Xe atoms<sup>55</sup>. By varying the collision energy over the energetic thresholds for

## Box 3: Synchrotron

Rather than confining molecules in a potential energy minimum at a single location in space as is done in a trap, molecules can also be confined in a minimum along a circle. The advantage of such a storage ring over a trap is that packets of particles with a non-zero mean velocity can be confined. While revolving in the ring, these particles can be made to interact repeatedly, at well-defined times and at distinct positions with electromagnetic fields and/or other particles.

A simple storage ring for polar molecules can be devised by bending an electrostatic hexapole into a torus. In the first experiments with such a prototype storage ring, beams of ammonia molecules were decelerated to a velocity of  $92 \text{ m s}^{-1}$ , bunched<sup>98</sup> and tangentially injected into the ring<sup>99,100</sup>, in which up to 50 distinct round trips could be observed. As a result of the longitudinal velocity spread, the packet of molecules gradually spreads out along the ring on making successive round trips, until they fill the entire ring. To counteract this spreading, a storage ring consisting of two half-rings separated by a 2 mm gap was constructed, as is schematically shown in Fig. B3a (ref. 101). By appropriately switching the voltages applied to the electrodes as the molecules pass through the gaps between the two half-rings, molecules experience a force that keeps them together in a compact bunch. This structure is the neutral analogue of a synchrotron for charged particles. Figure B3b shows the density of molecules stored in the ring as a function of storage time. It is seen that the width of the stored packet stays approximately constant. Bunching ensures a high density of stored molecules; in addition, it makes it possible to inject multiple—either collinear or counterpropagating—packets into the ring without affecting the packet(s) already stored.

different scattering channels, the threshold behaviour of the inelastic cross-sections could be accurately measured. Lower collision energies and a higher energy resolution can be obtained by two Stark-decelerated beams crossing at a  $90^\circ$  angle. In such a machine, bi-molecular inelastic or reactive scattering can be studied as a function of the collision energy, with an overall energy resolution down to better than  $1 \text{ cm}^{-1}$ . The combination of a crossed-beam machine with a molecular synchrotron (see Box 3 for details), in which multiple packets of molecules that revolve around the ring in opposite directions repeatedly interact, offers particularly interesting prospects for molecular-collision studies.

Ultimately, the precision in any spectroscopic measurement is limited by the interaction time of the particle to be investigated with the radiation field. In conventional molecular beam experiments, this interaction time is typically a few hundred microseconds. The ability to produce slow intense molecular beams significantly enhances the obtainable interaction time and hence resolution. The improved resolution can potentially be used for stringent tests of fundamental physics theories. For instance, polar molecules are being used to test violation of time-reversal symmetry<sup>56,57</sup>, in the search for a difference in transition frequency between chiral molecules that are each other's mirror image<sup>58</sup>, and for testing a possible time variation of the proton-to-electron mass ratio<sup>59,60</sup>. Recently, high-resolution microwave spectroscopy was carried out on Stark-decelerated beams of  $^{15}\text{ND}_3$  (ref. 61) and OH (ref. 62) molecules (Fig. 4). In these proof-of-principle experiments, an interaction time of up to a millisecond was obtained. To obtain

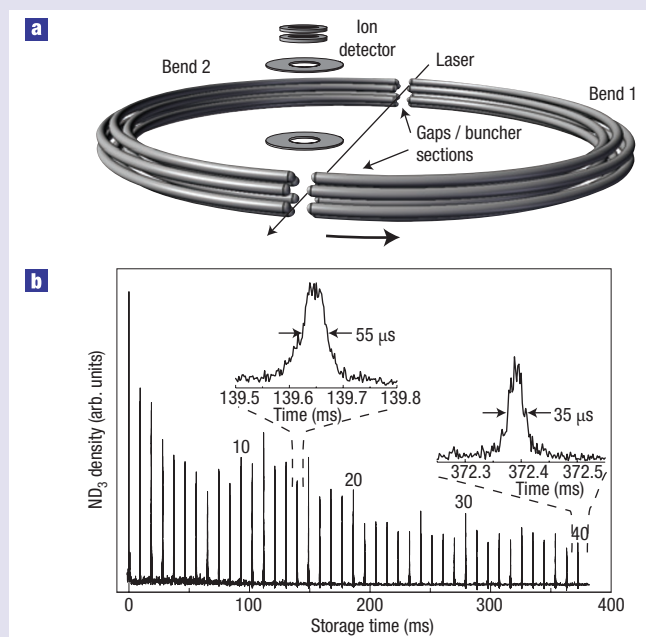


**Figure B3** The molecular synchrotron. **a**, The synchrotron consists of two hexapole half-rings with a 12.5 cm radius separated by a 2 mm gap. **b**, Density of ammonia molecules at the detection zone inside the synchrotron as a function of storage time up to the 40th round trip. Insets: Expanded views of two TOF profiles, more clearly illustrating the absolute widths of these peaks. Reprinted from ref. 101.

significantly longer interaction times, a molecular fountain can be used in which molecules are decelerated to a few metres per second, cooled and subsequently launched. The molecules fly upwards before falling back under gravity, thereby passing an interaction zone twice. The effective interrogation time in such a Ramsey-type measurement scheme includes the entire flight time between the two traversals. In this way an interrogation time of about one second can be obtained.

Trapped molecules can be investigated for several seconds. This long interaction time is of limited use to carry out high-resolution spectroscopy, as the molecules interact with the trapping field. However, it enables, for instance, accurate measurement of lifetimes of long-lived metastable states. The electrostatic trapping of molecules after Stark deceleration has been used to measure the lifetime of the first vibrationally excited  $X^2 \Pi$ ,  $v = 1$  state of OH, thereby benchmarking the Einstein  $A$  coefficients in the important Meinel system of OH (refs 63,64). The same experimental approach has been applied to accurately measure the lifetimes of CO molecules in the electronically excited metastable  $a^3 \Pi$  state<sup>31</sup>.

The ability to confine molecules in traps also holds great promise in the further development of the field of cold molecules. At sufficiently low temperatures, the de Broglie wavelength of the molecules becomes comparable to, or even larger than, the interparticle separation. In this regime, quantum degenerate effects dominate the dynamics of the particles, and a Bose–Einstein condensate can be formed. The anisotropic long-range dipole–dipole interaction is predicted to give rise to new and rich physics in these cold dipolar gases<sup>65–67</sup>, as has already

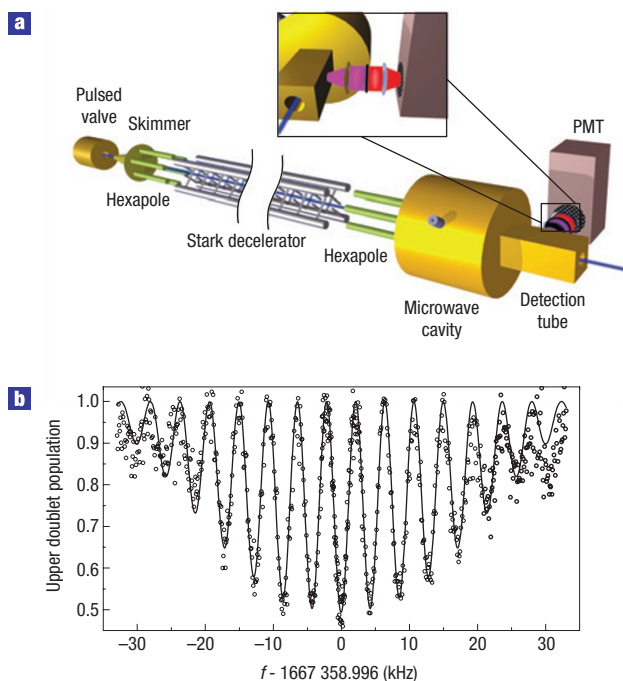


**Figure 4** High-resolution spectroscopy using Stark-decelerated beams. **a**, Schematic diagram of a microwave spectroscopy experiment at JILA in which a beam of OH radicals is Stark decelerated to  $200 \text{ m s}^{-1}$ , and interrogated in a 10-cm-long microwave cavity. PMT: Photomultiplier tube. **b**, Ramsey microwave spectroscopy for the transition between the  $F=2$  hyperfine states of the two  $\Lambda$ -doublet components of the rotational ground state of the OH radical. Reprinted with permission from ref. 62. © 2006 APS.

been observed in a Bose–Einstein condensate of chromium atoms with strong magnetic dipole–dipole interactions<sup>68,69</sup>. The strong electric dipole–dipole interactions also offer interesting prospects in quantum computation schemes<sup>70,71</sup>.

To experimentally study these phenomena, the temperature of the trapped sample of molecules needs to be further reduced. Various cooling schemes have been proposed to achieve temperatures below 1 mK. The most promising schemes are evaporative cooling, in which the molecules rethermalize after selective removal of the hottest molecules, and sympathetic cooling, in which the molecules are brought into contact with an ultracold atomic gas and equilibrate with it through elastic collisions. Another cooling scheme that is actively being pursued is cavity-assisted laser cooling<sup>72–75</sup>. Trap loss due to inelastic collisions, which transfer the molecules from the trapped low-field-seeking state to an anti-trapped high-field-seeking state, is expected to be severe in the first two cooling schemes. It is therefore essential to confine molecules in high-field-seeking states, eliminating the inelastic loss channels. An a.c. trap, in which a saddle-point electric field geometry is rotated fast enough to create a time-averaged potential well for high-field-seeking states, has already been demonstrated for ND<sub>3</sub> molecules<sup>76,77</sup>.

## CONCLUSIONS

The different tools that were developed in the past to transversally manipulate molecular beams, dating back to the Stern and Rabi era, have proven to be crucial for developments beyond molecular physics alone. The merging of molecular beam methods with those of accelerator physics now provides new tools to achieve complete

control over the full three-dimensional motion of molecules. Over the past few years, decelerators, lenses, bunchers, traps, storage rings and a synchrotron for neutral molecules have been demonstrated. Intense molecular beams with a tunable velocity and with a tunable width of the velocity distribution can now be produced. This new molecular beam technology is expected to become a valuable tool in a variety of chemical physics experiments, adding a new dimension to the long and rich history of the manipulation of molecular beams with external fields.

doi:10.1038/nphys1031

## References

1. Scoles, G. (ed.) *Atomic and Molecular Beam Methods* Vol. 1 & 2 (Oxford Univ. Press, New York, 1988 & 1992).
2. Gerlach, W. & Stern, O. Der experimentelle Nachweis der Richtungsquantelung im Magnetfeld. *Z. für Phys.* **9**, 349–352 (1922).
3. Rabi, I. I., Millman, S., Kusch, P. & Zacharias, J. R. The molecular beam resonance method for measuring nuclear magnetic moments. *Phys. Rev.* **55**, 526–535 (1939).
4. Friedburg, H. & Paul, W. Optische Abbildung mit neutralen Atomen. *Die Naturwissenschaften* **38**, 159–160 (1951).
5. Bennewitz, H. G. & Paul, W. Eine Methode zur Bestimmung von Kernmomenten mit fokussiertem Atomstrahl. *Z. Phys.* **139**, 489–497 (1954).
6. Bennewitz, H. G., Paul, W. & Schlier, Ch. Fokussierung polarer Moleküle. *Z. Phys.* **141**, 6–15 (1955).
7. Gordon, J. P., Zeiger, H. J. & Townes, C. H. Molecular microwave oscillator and new hyperfine structure in the microwave spectrum of NH<sub>3</sub>. *Phys. Rev.* **95**, 282–284 (1954).
8. Gordon, J. P., Zeiger, H. J. & Townes, C. H. The maser—New type of microwave amplifier, frequency standard, and spectrometer. *Phys. Rev.* **99**, 1264–1274 (1955).
9. Stolte, S. Reactive scattering studies on oriented molecules. *Ber. Bunsenges. Phys. Chem.* **86**, 413–421 (1982).
10. Wolfgang, R. Chemical accelerators. *Sci. Am.* **219**, 40–52 (1968).
11. Golub, R. *On Decelerating Molecules*. PhD thesis, MIT (1967).
12. Bromberg, E. E. A. *Acceleration and Alternate-Gradient Focusing of Neutral Polar Diatomic Molecules*. PhD thesis, Univ. Chicago (1972).
13. Bethlem, H. L., Berden, G. & Meijer, G. Decelerating neutral dipolar molecules. *Phys. Rev. Lett.* **83**, 1558–1561 (1999).
14. Maddi, J. A., Dinneen, T. P. & Gould, H. Slowing and cooling molecules and neutral atoms by time-varying electric-field gradients. *Phys. Rev. A* **60**, 3882–3891 (1999).
15. Bethlem, H. L., Berden, G., van Rooij, A. J. A., Crompvoets, F. M. H. & Meijer, G. Trapping neutral molecules in a traveling potential well. *Phys. Rev. Lett.* **84**, 5744–5747 (2000).
16. Bethlem, H. L., Crompvoets, F. M. H., Jongma, R. T., van de Meerakker, S. Y. T. & Meijer, G. Deceleration and trapping of ammonia using time-varying electric fields. *Phys. Rev. A* **65**, 053416 (2002).
17. van de Meerakker, S. Y. T., Vanhaecke, N., Bethlem, H. L. & Meijer, G. Higher-order resonances in a Stark decelerator. *Phys. Rev. A* **71**, 053409 (2005).
18. Gubbels, K., Meijer, G. & Friedrich, B. Analytic wave model of Stark deceleration dynamics. *Phys. Rev. A* **73**, 063406 (2006).
19. Bethlem, H. L. *et al.* Electrostatic trapping of ammonia molecules. *Nature* **406**, 491–494 (2000).
20. Bochinski, J. R., Hudson, E. R., Lewandowski, H. J., Meijer, G. & Ye, J. Phase space manipulation of cold free radical OH molecules. *Phys. Rev. Lett.* **91**, 243001 (2003).
21. van de Meerakker, S. Y. T., Smeets, P. H. M., Vanhaecke, N., Jongma, R. T. & Meijer, G. Deceleration and electrostatic trapping of OH radicals. *Phys. Rev. Lett.* **94**, 023004 (2005).
22. Hoekstra, S. *et al.* Optical pumping of trapped neutral molecules by blackbody radiation. *Phys. Rev. Lett.* **98**, 133001 (2007).
23. van de Meerakker, S. Y. T., Labazan, I., Hoekstra, S., Küpper, J. & Meijer, G. Production and deceleration of a pulsed beam of metastable NH ( $a^1\Delta$ ) radicals. *J. Phys. B* **39**, S1077–S1084 (2006).
24. Hudson, E. R. *et al.* Production of cold formaldehyde molecules for study and control of chemical reaction dynamics with hydroxyl radicals. *Phys. Rev. A* **73**, 063404 (2006).
25. Jung, S., Tiemann, E. & Lisdat, Ch. Cold atoms and molecules from fragmentation of decelerated SO<sub>2</sub>. *Phys. Rev. A* **74**, 040701(R) (2006).
26. Auerbach, D., Bromberg, E. E. A. & Wharton, L. Alternate-gradient focusing of molecular beams. *J. Chem. Phys.* **45**, 2160–2166 (1966).
27. Bethlem, H. L. *et al.* Alternating gradient focusing and deceleration of polar molecules. *J. Phys. B* **39**, R263–R291 (2006).
28. Bethlem, H. L., van Rooij, A. J. A., Jongma, R. T. & Meijer, G. Alternate gradient focusing and deceleration of a molecular beam. *Phys. Rev. Lett.* **88**, 133003 (2002).
29. Tarbutt, M. R. *et al.* Slowing heavy, ground-state molecules using an alternating gradient decelerator. *Phys. Rev. Lett.* **92**, 173002 (2004).
30. Wohlfart, K. *et al.* Alternating-gradient focusing and deceleration of large molecules. *Phys. Rev. A* **77**, 031404(R) (2008).
31. Gilijsse, J. J. *et al.* The radiative lifetime of metastable CO ( $a^1\Pi$ ,  $v=0$ ). *J. Chem. Phys.* **127**, 221102 (2007).
32. Hoekstra, S. *et al.* Electrostatic trapping of metastable NH molecules. *Phys. Rev. A* **76**, 063408 (2007).
33. Wing, W. H. Electrostatic trapping of neutral atomic particles. *Phys. Rev. Lett.* **45**, 631–634 (1980).
34. van Veldhoven, J., Bethlem, H. L., Schnell, M. & Meijer, G. Versatile electrostatic trap. *Phys. Rev. A* **73**, 063408 (2006).
35. Sawyer, B. C. *et al.* Magneto-electrostatic trapping of ground state OH molecules. *Phys. Rev. Lett.* **98**, 253002 (2007).
36. Vanhaecke, N., Meier, U., Andrist, M., Meier, B. H. & Merkt, F. Multistage Zeeman deceleration of hydrogen atoms. *Phys. Rev. A* **75**, 031402(R) (2007).
37. Hogan, S. D., Sprecher, D., Andrist, M., Vanhaecke, N. & Merkt, F. Zeeman deceleration of H and D. *Phys. Rev. A* **76**, 023412 (2007).
38. Hogan, S. D., Wiederkehr, A. W., Andrist, M., Schmutz, H. & Merkt, F. Slow beams of atomic hydrogen by multistage Zeeman deceleration. *J. Phys. B* **41**, 081005 (2008).
39. Narevicius, E. *et al.* An atomic coilgun: using pulsed magnetic fields to slow a supersonic beam. *New J. Phys.* **9**, 358 (2007).
40. Narevicius, E. *et al.* Stopping supersonic beams with a series of pulsed electromagnetic coils: an atomic coilgun. *Phys. Rev. Lett.* **100**, 093003 (2008).

41. Narevicius, E. *et al.* Stopping supersonic oxygen with a series of pulsed electromagnetic coils: A molecular coilgun. *Phys. Rev. A* **77**, 051401(R) (2008).
42. Yamakita, Y., Procter, S. R., Goodgame, A. L., Softley, T. P. & Merkt, F. Deflection and deceleration of hydrogen Rydberg molecules in inhomogeneous electric fields. *J. Chem. Phys.* **121**, 1419–1431 (2004).
43. Vliegen, E., Wörner, H. J., Softley, T. P. & Merkt, F. Nonhydrogenic effects in the deceleration of Rydberg atoms in inhomogeneous electric fields. *Phys. Rev. Lett.* **92**, 033005 (2004).
44. Vliegen, E., Hogan, S. D., Schmutz, H. & Merkt, F. Stark deceleration and trapping of hydrogen Rydberg atoms. *Phys. Rev. A* **76**, 023405 (2007).
45. Hogan, S. D. & Merkt, F. Demonstration of three-dimensional electrostatic trapping of state-selected Rydberg atoms. *Phys. Rev. Lett.* **100**, 043001 (2008).
46. Friedrich, B. & Herschbach, D. Alignment and trapping of molecules in intense laser fields. *Phys. Rev. Lett.* **74**, 4623–4626 (1995).
47. Zhao, B. S. *et al.* Molecular lens of the nonresonant dipole force. *Phys. Rev. Lett.* **85**, 2705–2708 (2000).
48. Stapelfeldt, H., Sakai, H., Constant, E. & Corkum, P. B. Deflection of neutral molecules using the nonresonant dipole force. *Phys. Rev. Lett.* **79**, 2787–2790 (1997).
49. Fulton, R., Bishop, A. I. & Barker, P. F. Optical Stark decelerator for molecules. *Phys. Rev. Lett.* **93**, 243004 (2004).
50. Barker, P. F. & Shneider, M. N. Slowing molecules by optical microlinear deceleration. *Phys. Rev. A* **66**, 065402 (2002).
51. Fulton, R., Bishop, A. I., Shneider, M. N. & Barker, P. F. Controlling the motion of cold molecules with deep periodic optical potentials. *Nature Phys.* **2**, 465–468 (2006).
52. Balakrishnan, N., Dalgarno, A. & Forrey, R. C. Vibrational relaxation of CO by collisions with <sup>4</sup>He at ultracold temperatures. *J. Chem. Phys.* **113**, 621–627 (2000).
53. Hutson, J. M. & Soldan, P. Molecule formation in ultracold atomic gases. *Int. Rev. Phys. Chem.* **25**, 497–526 (2006).
54. Bodo, E. & Gianturco, F. A. Collisional quenching of molecular ro-vibrational energy by He buffer loading at ultralow energies. *Int. Rev. Phys. Chem.* **25**, 313–351 (2006).
55. Gilijamse, J. J., Hoekstra, S., van de Meerakker, S. Y. T., Groenenboom, G. C. & Meijer, G. Near-threshold inelastic collisions using molecular beams with a tunable velocity. *Science* **313**, 1617–1620 (2006).
56. Hudson, J. J., Sauer, B. E., Tarbutt, M. R. & Hinds, E. A. Measurement of the electron electric dipole moment using YbF molecules. *Phys. Rev. Lett.* **89**, 023003 (2002).
57. Kawall, D., Bay, F., Bickman, S., Jiang, Y. & DeMille, D. Precision Zeeman–Stark spectroscopy of the metastable  $a(1)^2\Sigma^+$  state of PbO. *Phys. Rev. Lett.* **92**, 133007 (2004).
58. Daussy, Ch. *et al.* Limit on the parity nonconserving energy difference between the enantiomers of a chiral molecule by laser spectroscopy. *Phys. Rev. Lett.* **83**, 1554–1557 (1999).
59. Reinhold, E. *et al.* Indication of a cosmological variation of the proton–electron mass ratio based on laboratory measurement and reanalysis of H<sub>2</sub> spectra. *Phys. Rev. Lett.* **96**, 151101 (2006).
60. Shelkovich, A., Butcher, R. J., Chardonnet, C. & Amy-Klein, A. Stability of the proton-to-electron mass ratio. *Phys. Rev. Lett.* **100**, 150801 (2008).
61. van Veldhoven, J. *et al.* Decelerated molecular beams for high-resolution spectroscopy: The hyperfine structure of <sup>15</sup>ND<sub>3</sub>. *Eur. Phys. J. D* **31**, 337–349 (2004).
62. Hudson, E. R., Lewandowski, H. J., Sawyer, B. C. & Ye, J. Cold molecule spectroscopy for constraining the evolution of the fine structure constant. *Phys. Rev. Lett.* **96**, 143004 (2006).
63. van de Meerakker, S. Y. T., Vanhaecke, N., van der Loo, M. P. J., Groenenboom, G. C. & Meijer, G. Direct measurement of the radiative lifetime of vibrationally excited OH radicals. *Phys. Rev. Lett.* **95**, 013003 (2005).
64. van der Loo, M. P. J. & Groenenboom, G. C. Theoretical transition probabilities for the OH Meinel system. *J. Chem. Phys.* **126**, 114314 (2007).
65. Santos, L., Shlyapnikov, G. V., Zoller, P. & Lewenstein, M. Bose–Einstein condensation in trapped dipolar gases. *Phys. Rev. Lett.* **85**, 1791–1794 (2000).
66. Baranov, M., Dobrek, L., Góral, K., Santos, L. & Lewenstein, M. Ultracold dipolar gases—a challenge for experiments and theory. *Phys. Scr.* **T102**, 74–81 (2002).
67. Krems, R. V. Molecules near absolute zero and external field control of atomic and molecular dynamics. *Int. Rev. Phys. Chem.* **24**, 99–118 (2005).
68. Lahaye, T. *et al.* Strong dipolar effects in a quantum ferrofluid. *Nature* **448**, 672–675 (2007).
69. Koch, T. *et al.* Stabilization of a purely dipolar quantum gas against collapse. *Nature Phys.* **4**, 218–222 (2008).
70. DeMille, D. Quantum computation with trapped polar molecules. *Phys. Rev. Lett.* **88**, 067901 (2002).
71. André, A. *et al.* A coherent all-electrical interface between polar molecules and mesoscopic superconducting resonators. *Nature Phys.* **2**, 636–642 (2006).
72. Vuletić, V. & Chu, S. Laser cooling of atoms, ions, or molecules by coherent scattering. *Phys. Rev. Lett.* **84**, 3787–3790 (2000).
73. Domokos, P. & Ritsch, H. Mechanical effects of light in optical resonators. *J. Opt. Soc. Am. B* **20**, 1098–1130 (2003).
74. Morigi, G., Pinkse, P. W. H., Kowalewski, M. & de Vivie-Riedle, R. Cavity cooling of internal molecular motion. *Phys. Rev. Lett.* **99**, 073001 (2007).
75. Lev, B. L. *et al.* Prospects for the cavity-assisted laser cooling of molecules. *Phys. Rev. A* **77**, 023402 (2008).
76. van Veldhoven, J., Bethlem, H. L. & Meijer, G. AC electric trap for ground-state molecules. *Phys. Rev. Lett.* **94**, 083001 (2005).
77. Bethlem, H. L., van Veldhoven, J., Schnell, M. & Meijer, G. Trapping polar molecules in an ac trap. *Phys. Rev. A* **74**, 063403 (2006).
78. van de Meerakker, S. Y. T., Vanhaecke, N. & Meijer, G. Stark deceleration and trapping of OH radicals. *Annu. Rev. Phys. Chem.* **57**, 159–190 (2006).
79. Rangwala, S. A., Junglen, T., Rieger, T., Pinkse, P. W. H. & Rempe, G. Continuous source of translationally cold dipolar molecules. *Phys. Rev. A* **67**, 043406 (2003).
80. Rieger, T., Junglen, T., Rangwala, S. A., Pinkse, P. W. H. & Rempe, G. Continuous loading of an electrostatic trap for polar molecules. *Phys. Rev. Lett.* **95**, 173002 (2005).
81. Junglen, T., Rieger, T., Rangwala, S. A., Pinkse, P. W. H. & Rempe, G. Two-dimensional trapping of dipolar molecules in time-varying electric fields. *Phys. Rev. Lett.* **92**, 223001 (2004).
82. Tsuji, H., Okuda, Y., Sekiguchi, T. & Kanamori, H. Velocity distribution of the pulsed ND<sub>3</sub> molecular beam selected by a quadrupole Stark velocity filter. *Chem. Phys. Lett.* **436**, 331–334 (2007).
83. Deachapunya, S. *et al.* Slow beams of massive molecules. *Eur. Phys. J. D* **46**, 307–313 (2008).
84. Willitsch, S., Bell, M. T., Gingell, A. D., Procter, S. R. & Softley, T. P. Cold reactive collisions between laser-cooled ions and velocity-selected neutral molecules. *Phys. Rev. Lett.* **100**, 043203 (2008).
85. Patterson, D. & Doyle, J. M. Bright, guided molecular beam with hydrodynamic enhancement. *J. Chem. Phys.* **126**, 154307 (2007).
86. Maxwell, S. E. *et al.* High-flux beam source for cold, slow atoms or molecules. *Phys. Rev. Lett.* **95**, 173201 (2005).
87. Levy, D. H. The spectroscopy of very cold gases. *Science* **214**, 263–269 (1981).
88. Christen, W. & Rademann, K. Cooling and slowing in high-pressure jet expansions. *Phys. Rev. A* **77**, 012702 (2008).
89. Elioif, M. S., Valentini, J. J. & Chandler, D. W. Subkelvin cooling NO molecules via ‘billiard-like’ collisions with argon. *Science* **302**, 1940–1943 (2003).
90. Liu, N.-N. & Loesch, H. Kinematic slowing of molecules formed by reactive collisions. *Phys. Rev. Lett.* **98**, 103002 (2007).
91. Campbell, W. C., Tsikata, E., Lu, H.-I., van Buuren, L. D. & Doyle, J. M. Magnetic trapping and Zeeman relaxation of NH X<sup>2</sup>Σ<sup>-</sup>. *Phys. Rev. Lett.* **98**, 213001 (2007).
92. Moon, P. B., Rettner, C. T. & Simons, J. P. Rotor accelerated molecular beams. *J. Chem. Soc. Faraday Trans. II* **74**, 630–643 (1978).
93. Gupta, M. & Herschbach, D. A mechanical means to produce intense beams of slow molecules. *J. Phys. Chem. A* **103**, 10670–10673 (1999).
94. Gupta, M. & Herschbach, D. Slowing and speeding molecular beams by means of a rapidly rotating source. *J. Phys. Chem. A* **105**, 1626–1637 (2001).
95. Narevicius, E. *et al.* Coherent slowing of a supersonic beam with an atomic paddle. *Phys. Rev. Lett.* **98**, 103201 (2007).
96. van de Meerakker, S. Y. T., Vanhaecke, N., Bethlem, H. L. & Meijer, G. Transverse stability in a Stark decelerator. *Phys. Rev. A* **73**, 023401 (2006).
97. Meek, S. A., Bethlem, H. L., Conrad, H. & Meijer, G. Trapping molecules on a chip in traveling potential wells. *Phys. Rev. Lett.* **100**, 153003 (2008).
98. Crompvoets, F. M. H., Jongma, R. T., Bethlem, H. L., van Roij, A. J. A. & Meijer, G. Longitudinal focusing and cooling of a molecular beam. *Phys. Rev. Lett.* **89**, 093004 (2002).
99. Crompvoets, F. M. H., Bethlem, H. L., Jongma, R. T. & Meijer, G. A prototype storage ring for neutral molecules. *Nature* **411**, 174–176 (2001).
100. Crompvoets, F. M. H., Bethlem, H. L., Küpper, J., van Roij, A. J. A. & Meijer, G. Dynamics of neutral molecules stored in a ring. *Phys. Rev. A* **69**, 063406 (2004).
101. Heiner, C. E., Carty, D., Meijer, G. & Bethlem, H. L. A molecular synchrotron. *Nature Phys.* **3**, 115–118 (2007).

## Acknowledgements

The experiments described in this review that have been carried out in our laboratory are the result of almost ten years of research by a large group of people. We are greatly indebted to the students, postdocs, senior scientists and research technicians that have been involved in this work, and without whom these experiments would not have been possible. The measurements shown in Fig. 2a were carried out with the help of S. Hoekstra, J. J. Gilijamse and J. Küpper. H.L.B. acknowledges financial support from the Netherlands Organization for Scientific Research (NWO) through a VENI-grant. The fruitful collaboration and the open exchange of ideas with the other laboratories working in this area are greatly appreciated.

## Author information

Reprints and permission information is available online at <http://npg.nature.com/reprintsandpermissions>. Correspondence and requests for materials should be addressed to G.M.